World Applied Sciences Journal 6 (12): 1698-1704, 2009
ISSN 1818-4952

Flood Early Warning with Integration of Hydrologic and Hydraulic Models, RS and GIS (Case Study: Madarsoo basin, Iran)

Aliakbar Matkan, Alireza Shakiba, Hossain Pourali and Hamid Azari

Department of Remote Sensing and GIS, Earth Science Faculty, Shahid Beheshti University, Tehran, Iran

Abstract: Flood warning and forecasting could be one of the most effective non-structural procedures in managing floods that decreases the risks and disasters floods may cause. The main aim of this paper is to investigate the application of RS and GIS techniques associated with hydrological model related to flood forecasting. To achieve the aim, Madarsoo river basin as a flood prone region in Golestan province was selected. Since the rainfall on 10th August 2005 caused flood in the region, the images of NOAA/AVHRR satellite for the mentioned date was chosen to collect. Several distinguished stages were carried out during the research. First, all layers were prepared in GIS environment so that to be entered in Geo-database. Second, spatial database of parameters including; stream, cross sections, direction of runoff, banks and ModClark grid precipitation model were created and placed into the hydrologic model. In order to identify and classify clouds and estimate the rainfall data provided by NOAA/AVHRR, object-oriented classification and cloud indexing method were applied respectively. Next, the quantity of runoff caused by the rainfall was estimated by considering soil and land use maps and other inputs data in hydrologic model. Finally, to create the flood map, according to the topographical characteristics of the region, two most effective factors namely "The depth and speed of water" were taken from the hydrologic model and re entered to GIS environment. The results of the research indicated that we can achieve acceptable accuracy by using object-oriented classification, so that the overall accuracy of classification in this investigation is about 0.905 and Kappa coefficient is about 0.887. It was found that Cumulus congestus and Stratocumulus clouds with the rainfall rate of 10.8 mm/h and 2.2 mm/h, had the most and the least contribution to make floods. According to the hydrograph driven from the middle and down basins and also assuming that our estimation is done from the beginning of the rainfall, the flood map and the time in which the flood occurred could be predicted 20 and 33 hours before its peak.

Key words: flood early warning . rainfall estimation . hydrologic model . RS . GIS

INTRODUCTION

From 1960 to 1999, floods accounted for about one third of all natural catastrophes, caused more than half of all fatalities and were responsible for a third of overall economic losses [8]. In Iran, 1260 severe floods have occurred in the last four years, with annual average of 30 floods each year [20]. Also, based on scientific literature flood event is intensified nowadays. It is worthy to mention that many specific characteristics such as existence of Alborz and Zagros Mountains, aridity, intense rainfall in arid and semi arid areas, the lack of vegetation cover in most parts of the country and slope potentialize Iran as a suitable place for propagation of floods. Human activities, rapid urbanization and incorrect utilization of land in river catchment's district have served to be responsible for higher run-off and deteriorated river capacity problems. Hence, flood forecasting could be one of the most effective non-structural procedures in managing floods that decreases the risks and disasters floods may cause [20].

Conventional measurement of precipitation is not adequate for characterizing the areal variability of rainfall monitoring in most parts of the world, for ground-based measurement of precipitation is mostly a point-time event while precipitation itself is a time-space phenomena. Therefore, the new techniques such as satellite remote sensing are needed to be employed to complete the spatial distribution picture. In contrast to much conventional data, many satellite data have the advantage of near real-time data acquisition. Thus, during the last thirty years, satellites have proved to be able to provide improved rainfall data in both short-term and long-term records [18].

Corresponding Author: Hamid Azari, Department of Remote Sensing and GIS, Earth Science Faculty, Shahid Beheshti University, Tehran, Iran

Fig. 1: Sub basin map of case study (Madarsoo subbasin in Golestan province)

Many of scientists just have paid attention to rainfall estimating as the most principal factor for flood production with remotely sensed data. Among them we can refer to [2, 3, 6, 7, 9, 17, 19, 21].

Some of researchers have used radar data for rainfall estimation and integrated it with hydrological models for flood warning [4, 11, 15, 22]. Also some studies have led to flood warning and forecasting with integration of rainfall estimating by meteorological satellite data and hydrological models [5, 10, 14, 16].

In this study we focused on the using of remote sensing data, GIS, hydrological and hydraulic models with together for flood forecasting and mapping in madarsoo basin, golestan province.

CASE STUDY

The study area is Madarsoo basin in north-east of Iran that it's area is about 2400 km2 and located from 55° 21' to 56° 28' E (longitude) and from 36° 58'to 37° 30' N (latitude) (Fig. 1). In the basin, the heaviest rain occurred with 12-175 mm/day in 10 august 2005 leading to flood event. Therefore satellite images were used for that date.

MATERIALS AND METHODS

Materials: Satellite images used in the research, were obtained from Space Organization of Iran (SOI) and Remote Sensing and GIS faculty of Tabriz University. Also the maps and rainfall data were prepared from Forest, Range & Watershed Management Organization (FRWMO) and Water Research Institute (WRI), respectively.

Satellite images: The NOAA/AVHRR satellite images with 5 channels taken in 10 August 2005 by NOAA15 used for cloud classification and rainfall estimation.

Topographic maps: These files in 1:25000 scales were applied to produce digital elevation model as one of the most important inputs.

Stream map: The information of stream maps such as length and slope of river, outlet of basin, junctions, reaches and other physiographic information were entered to hydrological model.

Land use map: This map helps to specify the curve number maps and roughness coefficients used in hydrological and hydraulic models.

Soil hydrologic group map: To prepare curve number map, both land use and infiltration of soil information are needed. Soil hydrologic groups determine soil infiltration classes.

Rainfall gauges: For flood simulation, the information such as locations, density and homogeneity of stations, in 9, 10 and 11August 2005 and rainfall duration, were utilized.

Hydrometric gauges: The information of these gauges such as flow diagrams, observed stages and discharge hydrographs were applied to calibrate and optimize the hydrological and hydraulic models.

Methods: The framework of the operational integrating of Quantitative Precipitation Forecasting (QPF) with

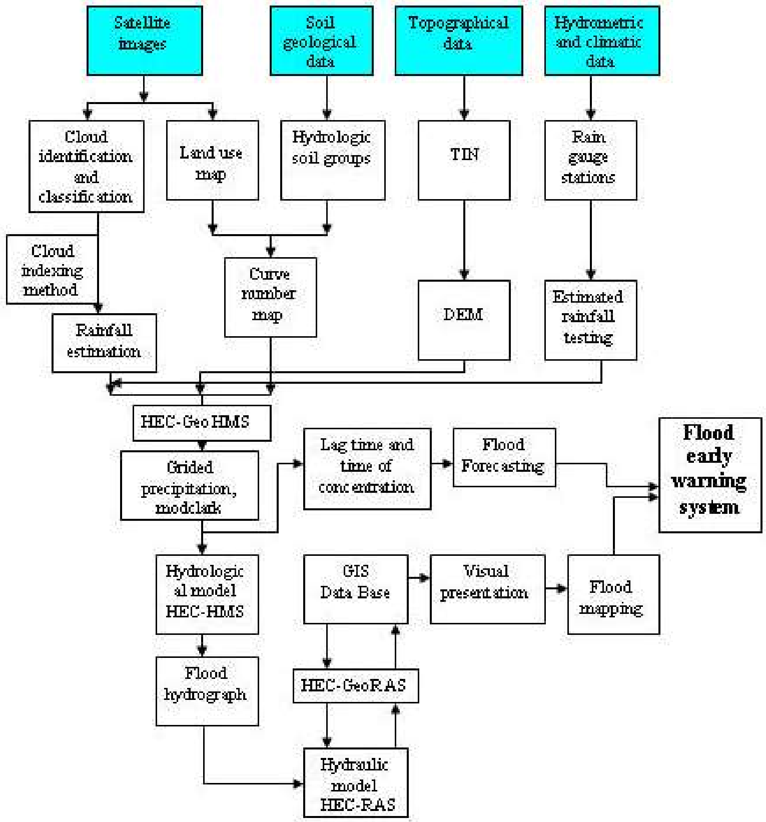

Fig. 2: Flowchart of study

HEC-HMS and HEC-RAS oriented GIS for inundation area mapping is illustrated in Fig. 2.

In the first part of the study, the atmospheric and radiometric corrections on the NOAA/AVHRR images were performed. Then these images were applied for classification of clouds through object oriented method. Although it has rather low spatial resolution (about 1.1 km in level 1b format), the temporal resolution of each satellite is about 12 hr daily which provides the real-time data required for the precipitation estimation. The object oriented classification was carried out by using Ecognition software and estimated the area of clouds in northeast of Iran. In object oriented classification, in addition to previous methods which consider visible comprehension and reflectance limits of clouds more, pattern and figure of clouds are also important. In present study, The Sixteen bands are produced with PCI Geomatica. The five main bands in satellite images and the other eleven bands such as Albedo and brightness temperature of main bands, solar zenith and azimuth angles, LST & SST, NDVI and deviation of nadir and cloud height are secondary bands. Form sixteen bands, 8 bands (like the 5 main bands and brightness temperature of band 3, 4 and cloud height) were selected and then classification was performed. In this

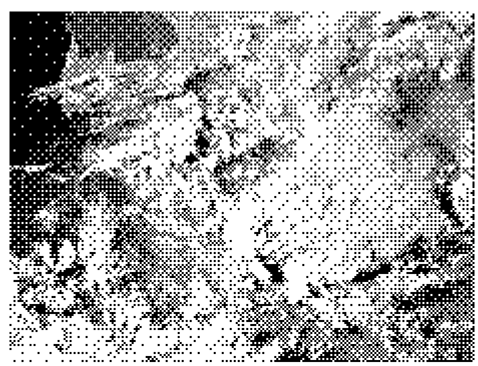

Fig. 3: Band 1 of AVHRR data

classification the seven cloud classes and one non-cloud class are obtained as follow:

1. Nimbostratus (Ns) 2.Cirrus (Ci) 3. Cumulonimbus (Cb) 4. Cumulus (Cu) 5. Cumulus congestus (Cg) 6. Strato cumulus (Sc) 7. Stratus (St) 8. Nocloud (terrain and sea).

Visible and Infrared bands and classified clouds are shown in Fig. 3-5, respectively.

Since the study area is too small to study cloud coverage, the entire Golestan province was selected (the total area is about 13050 Km2), just for rainfall

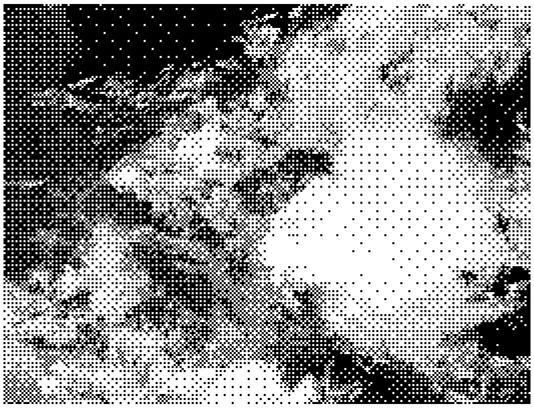

Fig. 4: Band 4 of AVHRR data

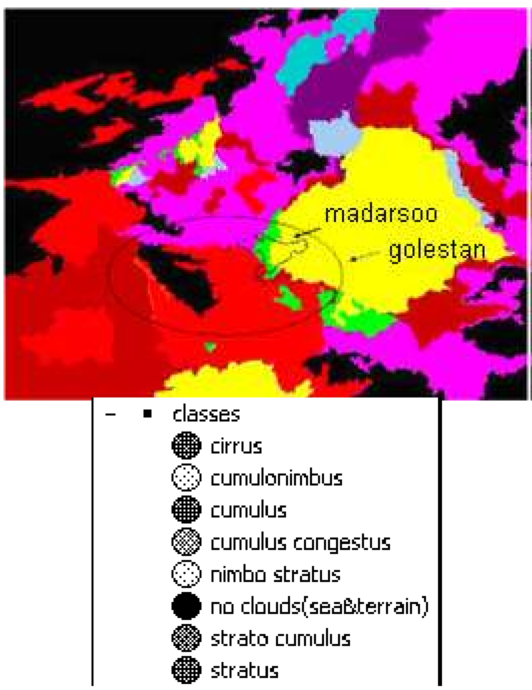

Fig. 5: Classified clouds in ecognition

estimation. As shown in Fig. 5, there are 5 cloud classes in Golestan province. The estimation of the average rainfall over the total basin and for each sub-division was carried out by using Thiessen's mean method [19].The eleven rain-gauges was used to generate ten polygons and through integrating satellite image and Thiessen polygons map, rain rate of each class was obtained by equation 1.

$$R = \frac{1}{A}\left(A_1 \times a + A_2 \times b + A_3 \times c + A_4 \times d + A_5 \times e\right) \quad (1)$$

where: A1, A2…, A5: number of pixels within seven cloud classes; R: Mean depth of rainfall estimated by Thiessen's method; a, b, …, e: constant coefficients; A: number of pixels within total area

Table 1: Estimated rain rates for each cloud type

Cloud type	Rain rate (mm/h)
Cumulus congestus	10.8
Cumulonimbus	8.1
Stratus	3.1
Cumulus	2.8
Stratocumulus	2.2

To find out the relative contribution of different cloud types to total precipitation of the area, it was necessary to divide theses constants into the duration (12 h in this case) so that to achieve the intensity of rainfall associated with each class [19]. Therefore the precipitation intensity using the cloud types can establish the relative contribution of each cloud type to the overall rainfall over the case study. Table 1 shows the precipitation intensities of each cloud class.

After obtaining rain rate of each cloud, the rainfall of sub-basins can be calculated from Barrett simple formula according to equation 2:

$$R = \left(\sum_{i=1}^{n} k_i \times A_i\right) \times \Delta t \quad (2)$$

where: i: the number of classes acquired from VIS-IR data; Ki: the rain rate of each class (mm/h); Ai: the percentage of each area for each class (%); R: the rainfall accumulation within sub-basin in Δt (mm); Δt: Rainfall duration (h).

During the next step, hydrological data was compiled to develop a GIS database in ArcGIS environment. GIS with combination of HEC-GeoHMS provides the essentials for river geometry. The gridded curve number was achieved from hydrological group and land use maps in HEC-GeoHMS. Then the lag time of subbasins calculated base on Curve Number method as equation 3:

$$Lag = \frac{\left(L^{0.8} \times (S+1)^{0.7}\right)}{\left(1900 \times Y^{0.5}\right)} \quad (3)$$

Where:

Lag: Sub basin's lag time (h)

L = Hydraulic length of sub basin (foot)

Y = Slope of sub basin (%)

S = Potential maximum retention obtained from equation 4: [12]

$$S = \frac{1000}{CN} - 10 \quad (4)$$

That CN is the Curve Number value

A watershed model which had been delineated by using DEM and HEC-GeoHMS was entered into HEC-HMS model. HEC-HMS is a rainfall-runoff model that providing various meteorological and hydrological processes to obtain flood hydrograph. Estimated rainfall data were entered into hydrologic model for mentioned storm using ModClark, a Quasi-distributed runoff procedure in HECHMS. This method needs gird-based precipitation file in HEC-HMS model. In this study the ModClark file is achieved by integration of subbasins and Standard Hydrologic Grid (SHG).

During next step, about 440 cross sections, left and right banks, main channel, runoff direction and bridges were entered into HEC-GeoRAS. HEC-GeoRAS in combination with HEC-RAS provides the tools for visual interpretation and evaluation of flood distribution and inundation maps. HEC-RAS is a hydraulic model that performs the flow analysis. Then, after importing the flood hydrographs estimated in HEC-HMS model, in steady flow, roughness coefficients and bridges information in HEC-RAS model, this model was runned and some information such as speed and depth of water in each cross section obtained. These information imported to GIS environment again and inundation map produced for visual interpretation and flood management.

RESULTS AND DISCUSSION

The Visible (VIS) channels 1 and 2 of the data were processed for albedo. The VIS image is used to identify cloud shapes, textures, organizational patterns and thicknesses. Then visible satellite data was compared to an IR image in order to determine the height of clouds. The NIR and IR channels 3, 4 and 5 of the data were processed for brightness temperature. All this information were assembled together and performed object oriented method with Ecognition software, consequently made reliable assessments of cloud types in image. Figure 3a and 3b show the visible and infrared bands respectively. The classified cloud is presented in Fig. 4. Although the coarse resolution of 1.1km of AVHRR data is not allowed for high-level classification, the object oriented classification was effective for the cloud type identification due to shape, texture and spectral information in classification process through the multi dimensional input object features [6]. From 5 detected clouds in Golestan province, there are 4 classes in Madarsoo basin which their areas are presented in Table 2.

After sample selection, TTA mask error (Fig. 6) was achieved. The Kappa coefficient is equal to 0.887 which is suitable in cloud classification and the overall accuracy was calculated about 0.905. It means that cloud classification is performed accurately.

Table 2: Cloud area and its percent

Cloud type	Area (km^2)	Area percent (%)
Cumulonimbus	1019	43.8
Cumulus congestus	791	34.0
Stratocumulus	299	12.9
Stratus	217	9.3
Sum	2326	100.0

Table 3: Rain rate and rain amount of each cloud type

Cloud type	Rain rate (mm/h)	Rain amount (mm)
Cumulus congestus	10.8	130
Cumulonimbus	8.1	97
Stratocumulus	3.1	37
Stratus	2.2	26

Since the rainfall duration was about 12 hours, the amount of rainfall for each cloud was calculated from the equation 5 as follow:

$$R = r^* \, 12 \text{ (h)} \tag{5}$$

R = the amount of rainfall for each cloud (mm)
r = rain rate of each cloud (mm/h)

Thus, the amount of rainfall and rain rate of each cloud in the study area and date mentioned was estimated as the Table 3:

It was found out that Cumuluscongestus and Stratocumulus clouds with the rainfall rate of 10.8 mm/h and 2.2 mm/h respectively, had the most and the least contribution to make floods.

HEC-GeoHMS divided basin into sub basins to enable an easy computation of runoff for each watershed. Gridded precipitation and ModClark process used to obtain the flood hydrograph in hydrologic model. The simulation period is 2 days, from 9th to 11th August 2005, in which heavy rainfall happened and provided Madarsoo River with high water level led to floods. Figure 7 shows the result of flood hydrograph and flow. As it is obvious in this figure, rising limb of observed hydrograph (black line) is approximately matched with calculated hydrograph (blue line). It is illustrated that rainfall characteristics such as rate, duration and steadiness are modeled well. But this fitting can't be seen in falling limb of observed and calculated hydrograph. Since falling limb is related to basin drainage [1], this unfitting can be due to inaccuracy of hydrologic soil groups or land use maps.

The lag time can be achieved from flood hydrographs which is equal to time distance between

Error Matrix based on TTA Mask

User \ Reference Class	cirrus	cumulonimbus	cumulus	cumulus congestus	nimbo stratus	strato cumulus	stratus	no clouds(sea&terrain)	Sum
Confusion Matrix									
cirrus	2730	179	58	0	0	93	0	0	3060
cumulonimbus	197	5093	0	11	0	0	0	0	5301
cumulus	143	0	1981	0	0	23	190	0	2337
cumulus congestus	0	0	0	1510	0	0	0	0	1510
nimbo stratus	0	0	0	0	630	0	83	0	713
strato cumulus	0	0	130	0	0	2926	175	0	3231
stratus	0	0	176	0	94	169	2801	384	3624
no clouds(sea&terrain)	0	0	0	0	0	0	348	5617	5965
unclassified	0	0	0	0	0	0	0	0	0
Sum	3070	5272	2345	1521	724	3211	3597	6001	
Accuracy									
Producer	0.889	0.966	0.845	0.993	0.87	0.911	0.779	0.936	
User	0.892	0.961	0.848	1	0.883	0.906	0.773	0.942	
Totals									
Overall Accuracy	**0.905**								
KIA	**0.887**								

reduce expand Close

Fig. 6: Error matrix and characteristic of classification

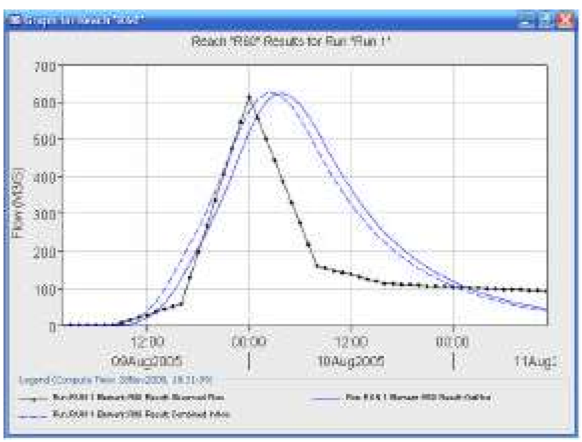

Fig. 7: Observed and calculated hydrograph in Tangrah station

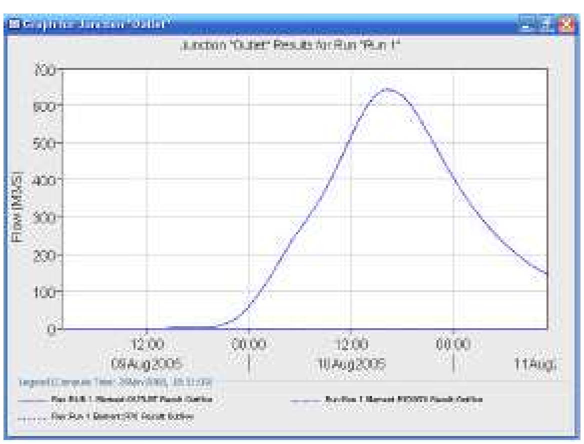

Fig. 8: Calculated hydrograph in outlet of basin

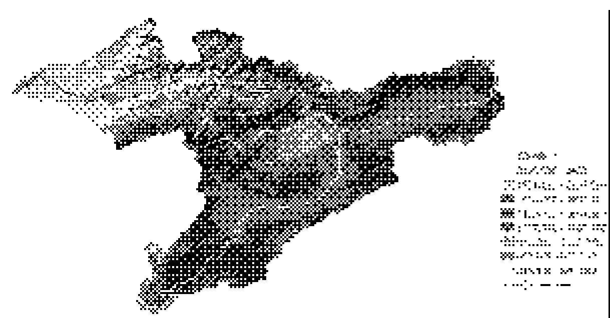

Fig. 9: Flood map in madarsoo basin

the middle of rainfall and crest segment of hydrograph. Hence, the lag time can be an important factor for flood forecasting. As is shown in Fig. 8, since the lag time of basin in the outlet of main river is about 33 hours (calculated using SCS CN method in HEC-GeoHMS), flood forecasting can performed about one day earlier.

The processing of data for HEC-RAS was carried out with flood hydrographs and HEC-GeoRAS exports such as cross sections, banks and flow paths and so on. The results of the simulation were gathered to the integrated ArcGIS for development and generation of flood inundation maps. The created inundation map by ArcGIS is shown in Fig. 9. The areas deluged by rainfall can be determined from throughout the map. Here, the flooded area stretches from Dasht and Ghizghale area to Golstan dam. The maximum extent of flood is determined about 2.5 kilometers which belongs to Kalaleh city. The reason could be related to over cutting of trees, mountain steep and incorrect urbanization.

CONCLUSION

The practical integration of remote sensing techniques and geographical information system was carried out with particular emphasis on suitability of semi-distributed hydrological modeling for execution of dependable flood simulation and early warning. In this study the developed operation is done for flood early warning and forecasting in Madarsoo basin. Object orient classification is a reliable technique for cloud classification. The near real-time NOAA/AVHRR data are processed for quantitative precipitation using cloud indexing modeling techniques. Precipitation estimates are then applied rainfall as input to a hydrological oriented GIS model. A set of HEC programs (GeoHMS, HMS, GeoRAS and RAS) and ArcGIS were used for runoff and water level simulation and generating the flood inundation maps. In conclusion, integration of Hydrologic and Hydraulic Models, RS and GIS can be a helpful strategy for Flood Early warning.

REFERENCES

1. Alizadeh, A., 2003. Principles of Applied Hydrology, Emam Reza (A) university, Mashhad, Iran.
2. Barrett, E.C. and D.W. Martin, 1981. The Use of Satellite Data in Rainfall Monitoring, Academic Press INC, New York.
3. Bayasgalan, M. and M. Erdenetuya, 1987. Estimation of cloud type, its amount and precipitation area using NOAA-AVHRR data.
4. Bedient, P.B., A. Holder, J.A. Benavides and B.E. Vieux, 2003. Radar-Based Flood Warning System Applied to Tropical Storm Allison. J. Hydrologic Engrg. 8 (6): 308-318.
5. Billa, L., Sh. Mansor, A.R. Mahmud and A.H. Ghazali, 2006. Modelling rainfall intensity from NOAA AVHRR data for operational flood forecasting in Malaysia. International Journal of Remote Sensing, 27 (23): 5225-5234.
6. Billa, L., Sh. Mansor and A.R. Mahmud, 2004. Quantitative Precipitation Forecasting Using Cloud-Based Techniques on AVHRR Data.
7. Budhakooncharoen, S., 2003. Rainfall Estimate for Flood Management Using Meteorological Data From Satellite Imagery.
8. Government of Germany, 2002. Early Warning, Forecasting and Operational Flood Risk Monitoring in Asia (Bangladesh, China and India). A Technical Report of Project (GT/1010-00-04).
9. Gonzalez, M.H. and I. Velasco, 1995. Rainfall area identification using satellite data. Climate Research, 5: 259-267.
10. Guleid, A. Artan, M. Restrepo and K. Asante, 2002. A flood early warning system for southern africa, Pecora 15/Land Satellite Information IV/ISPRS Commission I/FIEOS 2002 Conference Proceedings.
11. Hoblit, B.C. and D.C. Curtis, 2003. Integration of Radar Rainfall into Hydrologic Models.
12. Hydrologic Engineering Center, 2000. Geospatial Hydrologic modeling Extension (HEC-GeoHMS): User's manual. U.S. Army Crops of Engineers, Davis, CA.
13. http://www.class.ngdc.noaa.gov/saa/products/search?sub_id=0&datatype_family=AVHRR&submit.x=17&s ubmit.y=12
14. Kafle, T.P., M.K. Hazarica, K.G. Shresth, K. Prathumchai and L. Samarakon, 2006. Integration of remote sensing and GIS with flood simulation model for flood hazard mapping in the bagmati river, Nepal.
15. Knebl, M.R., Z.L. Yang, K. Hutchison and D.R. Maidment, 2005. Regional scale flood modeling using NEXRAD, rainfall, GIS and HEC-HMS\RAS: A Case study for the sun Antonio river basin summer 2002 storm event. Journal of Environmental Management, 75: 325-336.
16. Kwabena, O., A. Rodrigues, D. Macuacua, A. Guleid Artan, W. Ronald, Lietzow and P. James Verdin, 2007. Developing a Flood Monitoring System From Remotely Sensed Data for the Limpopo Basin. IEEE Transactions on Geoscience and Remote Sensing, Vol: 45 (6).
17. Lensky, I.M. and D. Rosenfeld, 1996. Estimation of Precipitation Area and Rain Intensity Based on the Microphysical Properties Retrieved from NOAA AVHRR Data. Journal of Applied Meteorology, Vol: 36.
18. Matkan, A.A., 1999. Passive Microwave Monitoring of Snow cover and Rainfall Over Iran, Using DMSP F-11 Special Sensor Microwave/ Imager Data, Ph.d Thesis, University of Bristol.
19. Mishra, J.K. and O.P. Sharma, 2001. Cloud top temperature based precipitation intensity estimation using INSAT-1D data. Int. J. Remote Sensing, 22 (6): 969-985.
20. Mohammadi, H., M. Maghsoudi and G.R. Roushan, 2007. Position and role of flood forecasting and warning systems in reduction of flood damages. Geographical Aspect Journal, No. 3, (In Persian).
21. Moesse, J. and E.C. Barrett, 1986. Interactive procedures for estimating precipitation from satellite imagery, Hydrologie Applications of Space Technology. Proceedings of the Cocoa Beach Workshop, Florida, August 1985. IAHS Publ. No. 160.
22. Plate, E.J. and I. Thanongdeth, 2003. Early Warning System for the Mekong River.